Tech Science Press

Experimental and Numerical Study of Structural Identification Using Non-Linear Resonant Decay Method

Mehdi Sarmast[1,*], Hamed Ghafari[2] and Jan R. Wright[3]

[1]Kennesaw State University, Department of Mechanical Engineering, MD 9075 840 Polytechnic Lane Marietta, GA 30060, USA.

[2]Malek Ashtar University of Technology, Department of Aerospace Engineering, Lavizan, Tehran 15875, Iran.

[3]School of Mechanical, Aerospace and Civil Engineering, University of Manchester, Manchester M13 9PL, UK.

[*]Corresponding Author: Mehdi Sarmast. Email: msarmast@kennesaw.edu.

Abstract: One of the practical approaches in identifying structures is the non-linear resonant decay method which identifies a non-linear dynamic system utilizing a model based on linear modal space containing the underlying linear system and a small number of extra terms that exhibit the non-linear effects. In this paper, the method is illustrated in a simulated system and an experimental structure. The main objective of the non-linear resonant decay method is to identify the non-linear dynamic systems based on the use of a multi-shaker excitation using appropriated excitation which is obtained from the force appropriation approach. The experimental application of the method is indicated to provide suitable estimates of modal parameters for the identification of non-linear models of structures.

Keywords: Non-linear modal identification; non-linear dynamic system; non-linear resonant decay method; force appropriation approach

1 Introduction

In practice, majority of structures represent some non-linear behaviour and there is significant interest in the identification of non-linear dynamic systems, particularly where they have multi degree of freedom (MDOF). Non-linear system identification is important not only for obtaining a better view of how the structure behaves with non-linear problems, but also for more accuracy in design with less safety factors. Identification involves a progression through detection, classification and finally estimation of a model that represents the system dynamics accurately. However, the process of model identification for non-linear systems is not as well developed as for linear systems, and a range of different model forms is associated with many different methods available. Currently there are several methods for non-linear identification in structural mechanics such as non-linear auto regressive moving average with exogenous inputs (NARMAX) model, higher order frequency response function (HFRF), non-linear normal modes (NNMs) and the non-linear resonant decay method (NL-RDM) [5].

The NARMAX model, which was suggested by Billings [1], is founded on distinct time and is a non-linear type of the distinct time ARMA model utilized in a few linear approaches. This model allows the measurement of greater order FRF. The largest part of the work up to now done by utilizing this model has been founded on individual input/output information and it sounds very much suitable for nearly low order complicated non-linear mechanisms. The created model does not easily allow to receive a significant physical parametric model and the inquiry of big order multi-input/multi-output mechanisms would include dealing with huge series of conditions.

The Higher Order Frequency Response Function (HFRF) may be achieved in a few approaches and is able to present a precious recognition of the existing basic non-linear mechanism in a system such as the organization and form of the non-linearity. Generally, using hypercurve fitting [4] may result in a

second order of usual and numerical equation in the physical counterparts. Nonetheless, this method is commonly imagined to be restricted to nearly low organization accumulated parameter mechanisms. Volterra Kernel [18] is the similar time shaper of the HFRF that grants the mechanism's response to e created by a number of convulsion integrals. Nonetheless, to present the HFRF, the Volterra series is usually utilized more.

A Non-linear Normal Mode (NNms) appears from an enforced non-linear change, which detaches the accepted equations of motion [10]. These 'modes' help recognise the non-linear conduct of the mechanisms [16,17]. They are different from the usual prototypal modes of the mechanism and are hard to be clarified based on the physical mechanism. There are some approaches to clarify these non-linear modes which are to be improved. Meeting several fitting criteria by these approaches founded on this representation seems unlikely. A connected approach, Proper Orthogonal Decomposition [7], plans to break up the non-linear mechanism into its combining feature forms, but it does not give a complete and appropriate pattern to grant the earlier planed standards. Using NNMs in non-linear mechanism recognition has been formulated but it is not still in practice.

An ideal non-linear system identification method would be applicable to continuous as well as lumped parameter systems, with MDOF. It would be able to cope with many modes and yield a Multiple Input - Multiple Output (MIMO) model, i.e., to be able to use many different shakers to excite a structure simultaneously at different locations. The ideal non-linear system identification method should allow comparison with other models in physical space, including for instance finite element models, and should be understandable by the practicing engineer. It should work for any non-linearity and ideally allow the type and location of any non-linear element to be determined.

The focus of this paper is upon non-linear identification of structures which can be identified using linear modal testing methods but indicate some non-linear effects. For such systems normal modes of vibration represent the underlying linear behaviour. The NL-RDM approach explored in this work was introduced by Wright [19,20]. It plans to determine a pattern founded on linear modal space, the supposed expanded modal pattern [12]. It is basically founded on the expansion of the authentic recovering force surface method in modal space [9] and benefits from the procedures for the usual mode force provision [21].

The NL-RDM is the first method to suggest the use of appropriated excitation to non-linear systems in order to restrict the number of responding modes. In fact, the identification complexity is reduced by using appropriated force patterns because it makes a filter in which mode of interest is driven more than other modes.

It is helpful to consider that modes can be divided into the following categories [15,20]: (1) modes that are linear, (2) modes that behave non-linearly but having no significant non-linear coupling to other modes, (3) modes that behave non-linearly but having significant non-linear coupling to other modes. A modal model based on the above categories would be simpler than a fully coupled non-linear model covering all the modes because of the limitation in the number of coupling terms.

It should be noticed that typically 60%-70% of the modes of most complex non-linear structures would behave in the linear categories as proportionally damped where reasonably accurate identification using classical linear methods is possible. However, the remainder of modes could benefit from an identification process targeted at estimating key terms in the extended modal model, namely linear cross coupling terms, direct non-linear terms and non-linear cross coupling terms [3]. Thus the philosophy of NL-RDM is to identify a modal model where some of the modes behave linearly and the rest behave non-linearly; the number of coupling terms would therefore be minimised.

The NL-RDM approach allows for non-linear cross coupling and it can be important in identifying a non-linear structure because any non-linear mathematical model used for the identification must allow for non-linearly coupled modes. Moreover, the NL-RDM utilizes the results coming from burst excitation in the non-linear curve-fitting. The method includes exciting the structure with a burst sine at the natural frequency of the mode of interest; after finishing the burst excitation, the results are granted to decompose openly. The entire force and response signals are utilized to do the non-linear identification of the mode.

As only the appropriated mode and the modes that are non-linearly coupled to it respond, the identified non-linear model is of low complexity and the number of candidate terms is low.

The NL-RDM was applied successfully to a number of simulated systems and experimentally to a clamped panel structure and also a wing structure. In this work, the NL-RDM approach is illustrated in a non-linear simulated system and an experimental rig structure to determine how well this method can identify such non-linear dynamic systems. Also, this is the first time that the effects of inaccuracy in mode shapes, force vectors, natural frequencies and sensitivity to noise are investigated. This paper is organized as follows: In Section 2, a complete explanation of the NL-RDM is presented. Numerical and experimental results are presented in Sections 3 and 4. Conclusions are discussed in Section 5.

2 Methodology for Non-Linear Resonant Decay Method

In this section, the theoretical basis of this approach will be described. To make the identification of continuous multi-degree-of-freedom of non-linear systems possible, the identification growth happens in linear modal space. Provided that the modal matrix of the underlying linear system is possible to be identified, then it is likely to transform the measured responses and forces from physical to modal space [15].

2.1 Basic Equations

The equations of motion in physical space for a dynamic system which have been discretized as N DOF including stiffness non-linearity are:

$$[M]\{\ddot{w}\}+[C]\{\dot{w}\}+[K_L]\{w\}+[K_{NL}]\{w\}=\{F(t)\} \tag{1}$$

where $[M]$ is the mass matrix, $[C]$ is the damping matrix, $[K_L]$ is the linear stiffness matrix, $[K_{NL}]$ is the non-linear stiffness matrix, $\{F(t)\}$ is the vector of applied nodal forces, and $\{w(t)\}$ is the vector of physical displacements. The transformation between physical and modal space is defined by

$$\{w(t)\}=\sum_{r=1}^{N}\{\phi\}_r p_r(t)=[\phi]\{p(t)\} \tag{2}$$

where $\{p(t)\}$ is a vector of modal amplitudes, and $[\phi]$ is the modal matrix of the N modes $\{\phi\}_r$, r = 1, 2… N of the underlying linear system, which may be obtained by solving the classical eigenvalue problem for un-damped free vibration. The corresponding un-damped natural frequencies are ω_r (r = 1, 2… N). Substituting the modal expansion Eq. (2) for the system equations of motion Eq. (1), pre-multiplying by $[\phi]^T$ and also using the orthogonality of the modes, this equation of motion in modal space becomes

$$[m]\{\ddot{p}\}+[c]\{\dot{p}\}+[k_L]\{p\}+\{f_{NL}\}=\{f(t)\} \tag{3}$$

where the modal mass matrix $[m]$ and linear modal stiffness matrix $[k_L]$ are diagonal and the modal damping matrix $[c]$ is diagonal for proportionally damped systems. $\{f(t)\}$ is the applied modal force vector and $\{f_{NL}\}$ is the vector of non-linear restoring forces in modal space. Clearly, in order to be able to perform this transformation, the modal matrix is assumed to be known from low force level results. For a particular mode of a proportionally damped non-linear system, Eq. (3) is in the form of a single degree of freedom system, namely

$$m_r\ddot{p}_r+c_r\dot{p}_r+k_r p_r+f_{r,NL}=f_r(t) \tag{4}$$

where p_r is the rth modal displacement. m_r , c_r and k_r are the rth mode modal mass, damping and stiffness, and $f_r(t)$ is the corresponding applied modal force. The modal mass and stiffness for the linear system are related by the un-damped natural frequency from the equation $k_r = m_r \omega_r^2$ .The term $f_{r,NL}$ refers to the rth mode non-linear modal restoring force and in general includes other modal coordinates to allow non-linear cross coupling.

2.2 Classify Linear and Non-Linear Modes

A modal test with multi-exciters and random (or multi-sine) excitation is performed at several excitation levels as a check on homogeneity. Reciprocity could also be examined. It is anticipated that some modal peaks will exhibit non-linear effects at some levels of force and that some others will be largely unaffected by an increase in excitation level. The modes may then be classified as 'linear' or 'non-linear'. It would be useful to develop indicator functions that would allow linear and non-linear modes to be recognised. A suitable excitation level for obtaining an essentially linear FRF matrix is then selected and the result used in the next stage of the method.

2.3 Modal Parameters Identification of Underlying Linear System

The FRF matrix measured at a low excitation level is used to estimate the modal parameters (i.e., natural frequency, damping, mode shape and modal mass) for the underlying 'linear' modes using a curve fitting approach. In many cases, the mode shapes are sufficiently and accurately identified using such a phase separation method. However, in some cases a force appropriation approach may be more accurate. In this case, the FRF matrix may be used to estimate the appropriated force vector for each mode.

2.4 Modal Parameters Identification of Underlying Linear System

The Multivariate Mode Indicator Function (MMIF) [21] is then calculated from the low level FRF matrix and appropriated force vectors determined for each mode of interest (i.e., those affected by non-linearity). It is important to use a suitable choice of number and location of exciter positions. As an alternative approach to curve fitting, the mode shape may then be estimated by normal mode tuning, either performed on the structure itself at low level excitation ('hard' tuning) or preferably using the FRF matrix to represent the system ('soft' tuning). All modes in the range of interest need to be included in the mode shapes identified. Additionally, for any mode that was seen to behave linearly in the homogeneity test and was proportionally damped, the estimated modal parameters (i.e., modal mass, damping and stiffness) may be used in the final model and no more action was taken. However, parameters for modes that behaved non-linearly will need to be identified separately using NL-RDM.

2.5 Normal Mode Tuning to Determine Voltage Patterns

Once it is clear that the system is behaving linearly at a low level of excitation, each mode can be tuned using the LMS normal mode tuning software or by multiplying the appropriated force vectors in the imaginary part of the FRF matrix. As described in the previous sub-section, the appropriated force vectors are now known. Normal mode tuning is then performed, i.e., the appropriated force pattern is applied and the frequency varied until the forces and responses are approximately 90° out of phase (phase resonance condition). The corresponding voltage amplitudes and phases for the tuned condition were recorded to be used in the burst application; this is because the shaker/structure interaction introduces a variable frequency gain and phase lag between the drive voltages and the measured forces.

2.6 Application of Force Burst and Measurement of Physical Response

The appropriated force vector is then applied as a 'burst' sine to each of these 'non-linear' modes in turn, at a level which is great enough to excite any non-linear behaviour present. A burst sine is an

excitation signal that involves applying a sine wave to the system for a given time and then removing it. The burst sine amplitude is ramped up at the start and down at the end to avoid exciting significant transient. This approach was first used in the RDM [6,8,11] and allows building up the response to a steady-state and then after removing the excitation, the system response dies away within the measurement window. Supposing that force and response signals are measured from time 0 to time t_i, a burst excitation begins at the time example of t_a and ends at the time example of t_b, in a place that $0 < t_a < t_b < t_i$. A burst sine [13,14] of the rth mode is given by the equation

$$f_r(t) = \begin{cases} \dfrac{A_0}{t_a} t \sin \omega_r t & t < t_a \\ A_0 \sin \omega_r t & t_a < t < t_b \\ A_0 (1 - \dfrac{t - t_b}{t_i - t_b}) \sin \omega_r t & t_b < t < t_i \end{cases} \tag{5}$$

where A_0 is the amplitude of excitation and ω_r is the undamped natural frequency of the rth mode of the underlying linear system. If the mode is uncoupled non-linearly, then the appropriated mode should dominate the response in the steady-state phase. If it is non-linearly coupled, other modes may also exhibit a significant response.

The idea of using the appropriated sine is that only one or a limited sub-set of modes is excited and so the identification model is of reasonably low order. The reason for using the burst is that leakage errors may be minimised when performing integrations or differentiations. Often the force vector is unable to isolate the mode of interest perfectly. For a linear system, this can occur if too few exciters are used or if the exciters are not optimally placed. In practice, the number of exciters required should equal the effective number of modes around a natural frequency of interest. For a non-linear system, imperfect appropriation will also occur if a force vector, evaluated from an FRF generated at a low force level, behaves differently at a higher force level i.e., the FRF is different. Any changes due to amplitude are expected to affect the modes in the region of the mode behaving non-linearly. Thus if the relevant modes are included in the regression, the identification should account for other modes excited close in frequency as for a linear system.

2.7 Transformation to Modal Space and Identification

The physical force, acceleration, velocity and displacement were transformed to modal space using the mode shapes identified earlier to prepare for curve fitting, so the force vector in modal space is determined when the transposed modal matrix is used to pre-multiply the force vector in physical space.

Least square is a numerical method which can be used to estimate the model parameters. One of the difficulties with any identification method is to decide which terms in the polynomial series representing the non-linear stiffness (or damping) contribution should be included in the final system model. There are two possible approaches [2] to obtain a reduced order model for any given curve fit to a set of modal data. Firstly, all possible terms up to a certain order may be included and then terms with the least contribution to the response is discarded until a defined goodness of fit is achieved, Backward Elimination (BE). In other words, it begins with a model containing all the independent variables of interest. Then, at each step the variable with the smallest contribution is deleted. Alternatively, terms may be added to the model on the basis of providing maximum contribution to the response until the desired goodness of fit is reached, Forward Selection (FS). In other words, Forward Selection starts with an empty subset to which one basis function is added at a time, the one which mostly reduces the sum of squares error until some chosen criterion is reached.

The mean square error function (MSE) was used to compare the effectiveness of two different approaches to least squares curve fitting as the model order was allowed to change. The function demonstrates the ability of each method to accurately identify a system by curve fitting, which is

especially important when allowing for non-linear terms in the system. The MSE [13] is found through the equation

$$MSE = \frac{1}{n}\sum_{i=1}^{n}\left(\frac{(T_i - I_i)}{T_i}\right)^2 \tag{6}$$

where T and I represent true data and the response data generated for the identified model. Having identified modal parameters for any linear modes using linear methods and the linear/non-linear modal parameters using the NL-RDM, the parameters may be assembled to obtain a set of modal equations that should represent the system over the frequency range of interest. The identified parameters, obtained through linear or non-linear curve fitting methods, should be checked in some general manner to validate the model. The modal equations assembled from the initial linear and non-linear test phases may be used to check the ability of the final model to reproduce a measured forced response on the real structure; ideally, a signal different to that used for the identification such as random, stepped sine or chirp excitation should be employed.

3 Numerical Example

In this section, the application of NL-RDM will be simulated for a 2 DOF system with hardening cubic stiffness of non-linearity. Non-linear element is positioned between the first mass and ground and causes both of the modes to be coupled and non-linear. Sensitivity of NL-RDM is tested further by the introduction of the following types of measurement errors; mode shape errors, force vector errors, natural frequency errors and sensitivity to noises. The equations of motion in physical space for the 2DOF non-linear system shown in Fig. 1 can be written as

$$\begin{bmatrix} M_1 & 0 \\ 0 & M_2 \end{bmatrix}\begin{Bmatrix} \ddot{w}_1 \\ \ddot{w}_2 \end{Bmatrix} + \begin{bmatrix} C_1 + C_2 & -C_2 \\ -C_2 & C_2 + C_3 \end{bmatrix}\begin{Bmatrix} \dot{w}_1 \\ \dot{w}_2 \end{Bmatrix} + \begin{bmatrix} K_1 + K_2 & -K_2 \\ -K_2 & K_2 + K_3 \end{bmatrix}\begin{Bmatrix} w_1 \\ w_2 \end{Bmatrix} + \begin{Bmatrix} K_{NL} w_1^3 \\ 0 \end{Bmatrix} = \begin{Bmatrix} F_1 \\ F_2 \end{Bmatrix} \tag{7}$$

where $M_1 = M_2 = 1$ kg, $C_1 = C_3 = 1.6$ Ns/m and $C_2 = 0.3$ Ns/m, $K_1 = K_3 = 2000$ N/m, $K_2 = 1000$ N/m and K_{NL}=1.00e9 N/m^3.

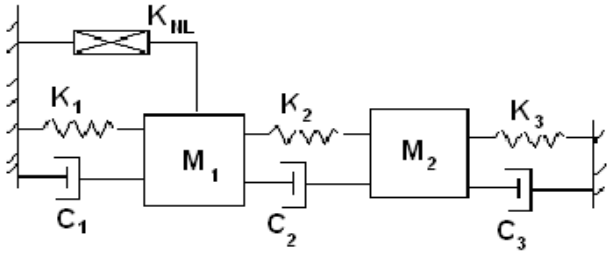

Figure 1: 2DOF system with grounded cubic stiffness non-linearity

This equation of motion in physical space yielded the exact mode shapes of the underlying linear system as {1, 1} and {1, -1} because of the present symmetry. The corresponding exact linear natural frequencies are 7.118 Hz and 10.066 Hz respectively. Note that the damping is proportional, being a combination of the mass and stiffness matrices, namely [C] = [M] + 0.0003*[K]. Transforming Eq. (6) to linear modal space yields two coupled modal equations, namely

$$\begin{bmatrix} 2 & 0 \\ 0 & 2 \end{bmatrix}\begin{Bmatrix} \ddot{p}_1 \\ \ddot{p}_2 \end{Bmatrix} + \begin{bmatrix} 3.2 & -c_2 \\ -c_2 & 4.4 \end{bmatrix}\begin{Bmatrix} \dot{p}_1 \\ \dot{p}_2 \end{Bmatrix} + \begin{bmatrix} 4000 & 0 \\ 0 & 8000 \end{bmatrix}\begin{Bmatrix} p_1 \\ p_2 \end{Bmatrix} + \begin{Bmatrix} 1e9(p_1^3 + p_1^2 p_2 + p_1 p_2^2 + p_2^3) \\ 1e9(p_1^3 + p_1^2 p_2 + p_1 p_2^2 + p_2^3) \end{Bmatrix} = \begin{Bmatrix} f_1 \\ f_2 \end{Bmatrix} \tag{8}$$

Fig. 2 shows the presence of non-linearity in both modes by indicating the shift in the FRF peaks for both modes at different levels of force to check homogeneity.

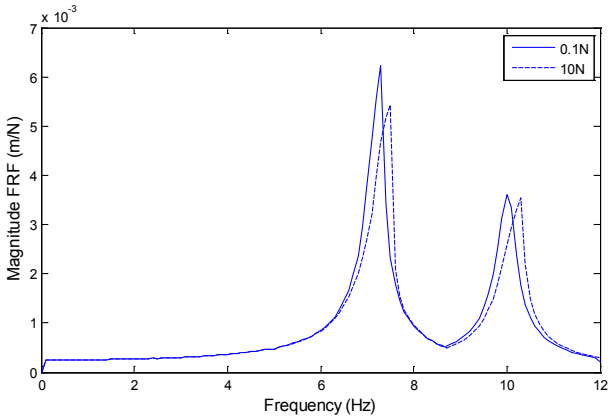

Figure 2: FRF to stepped sine excitation at low and high force levels

The eigenvalue MMIF based on the known physical model is shown in Fig. 3 and the eigenvalue drops to nearly zero; these low minima indicate the natural frequencies but also indicate better appropriation of those modes. The eigenvectors corresponding to each minimum are {1, 1} and {-1, 1} respectively.

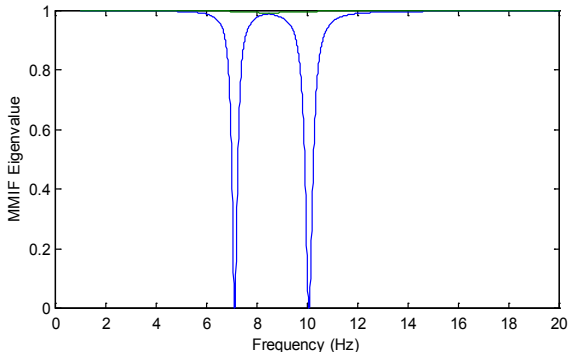

Figure 3: MMIF for 2DOF system with two exciters

These force vectors may be used to determine the linear mode shapes by soft tuning; the force vector would be multiplied by the imaginary part of the FRF matrix. Results for these exact mode shapes are shown in Fig. 4.

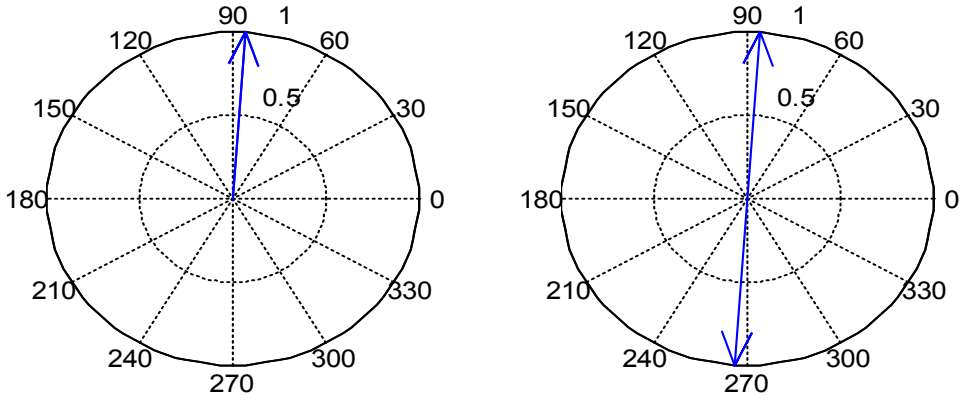

Figure 4: Scatter diagrams showing mode shapes determined by soft tuning FRF

A burst is applied to each of the modes with the relevant appropriated force vector. The burst length is 30 seconds and there are 6000 data points. The excitation is removed after 50% of the measured

window. The data are transformed from physical into modal space using the modal matrix. The first and second modes are excited using their appropriated forces and Figs. 5 and 6 show the modal force and acceleration in both modes. The results clearly indicate some level of non-linear coupling between the two modes.

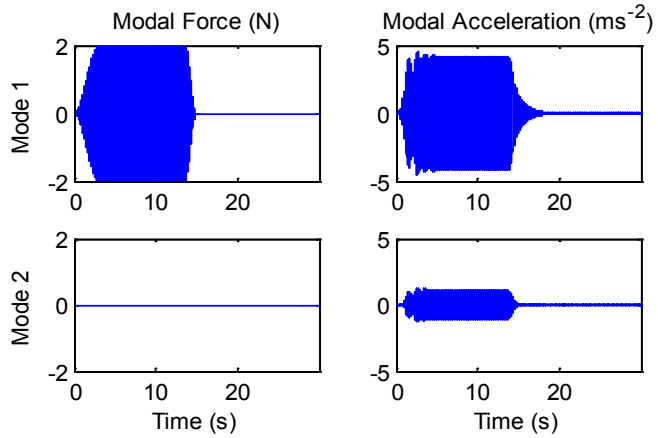

Figure 5: Modal force and acceleration when first mode is excited using burst

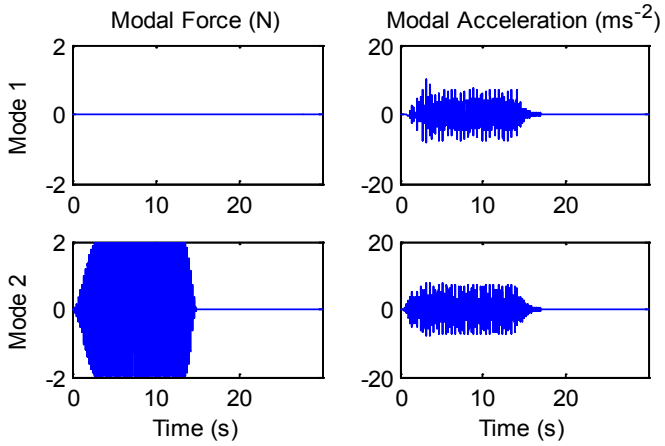

Figure 6: Modal force and acceleration when second mode is excited using burst

Least Squares curve fitting is used to identify parameters. So, the two modes are identified and tabulated in Tab. 1, which included modal linear and non-linear direct and coupled terms for both modes. The results indicate excellent agreement between true and identified parameters.

Table 1: Comparison between true and identified parameters for both modes

Parameter	First mode		Second mode	
	True	Identified	True	Identified
m (kg)	2.00	2.00	2.00	2.00
c (kg/s)	3.20	3.20	4.40	4.40
k (N/m)	4000	4000	8000	8000
k Cubic (3,0)	1.00e + 9	1.00e + 9	1.00e + 9	1.00e + 9
k Cubic (2,1)	3.00e + 9	3.00e + 9	3.00e + 9	3.00e + 9
k Cubic (1,2)	3.00e + 9	3.00e + 9	3.00e + 9	3.00e + 9
k Cubic (0,3)	1.00e + 9	1.00e + 9	1.00e + 9	1.00e + 9

3.1 Inaccuracy in Mode Shape

Consider the effect of the mode shapes upon the identification process. The modal matrix is used to transform the data measured in physical space into the modal space corresponding to the underlying linear system, prior to the curve fitting process. If a perfect modal matrix is available, then it is possible to transform these equations into modal space without error. However, if one or more mode shapes contain errors then the transformation will be imperfect. The effect of an imperfect modal matrix upon the applied modal force vector would be to convert the physical applied force vector into the imperfect 'modal' space. Since the appropriated force vectors expressed in physical space will still be perfect, each will have the desired effect on the true system as intended, because the underlying physical equations have not changed. However, the imperfect modal transformation will mean that the responses in the transformed 'modal' space will be mixed up to a degree.

To examine the errors caused by the mode shape inaccuracy, an error of up to 20% is added to the mode shape value for the first mode. The NL-RDM is applied as usual to the system to estimate the non-linear modal parameters from the incorrect modal data. Finally, these new parameters are plotted against the level of inaccuracy in the mode shape for both of the modes; for a better view of the degree of inaccuracy, a vertical or horizontal line is placed through the zero error positions or in some other graphs the grid is left on. Variations of modal mass, damping and stiffness with inaccuracies in mode shape are shown in Figs. 7(a), 7(b) and 7(c) respectively. The results show how inaccuracy in the estimated mode shape influences the identified parameters. Also, Figs. 7(d) and 7(e) illustrate the sensitivity of the coefficient of cubic stiffness non-linearity in the first and second mode respectively; the errors in these terms are greater than on the linear stiffness terms.

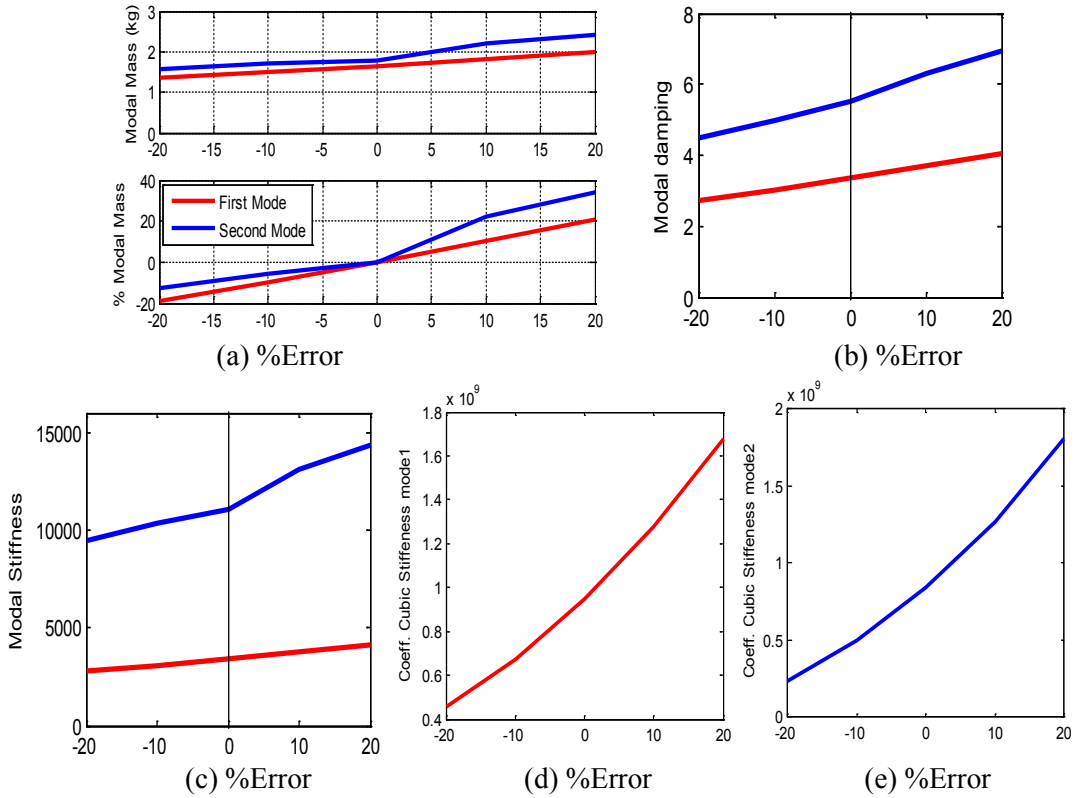

Figure 7: Variations with inaccuracy on mode shape-red (mode 1) and blue (mode 2) a) modal mass b) modal damping c) modal stiffness d) cubic stiffness non-linearity on mode 1 e) cubic stiffness non-linearity on mode 2

3.2 Inaccuracy in Force Vector

Force vectors are calculated from the underlying linear FRF or MMIF of the system, normally obtained at a low level of excitation. It is then used for the burst excitation of the system, to gather system data for the analysis of the system using the NL-RDM. The force vector referred to is the force generated by the shakers, in order to generate vibration in the system. In a linear system, force vectors are chosen for application at a specific location, and in a specific direction, in order to isolate and vibrate a single specified normal mode. Due to coupling effects within non-linear systems, other modes may also be vibrated. However, appropriated force vectors are still employed, as this reduces the response in those modes. It is still assumed that all other parameters are accurate, including the natural frequency, mode shape etc., and that the remainder of the test process is carried out perfectly. The aim is to try to isolate the effect of the force vector inaccuracy as much as possible. The inaccuracy is expressed as a percentage of the magnitude of the force vector. This new force vector is applied to the system for various values of errors between ± 20%. An error of up to 20% is added to the correct force vector. The NL-RDM is applied as usual to the system to estimate the modal parameters from the incorrect force vector. Hence, these new parameters are plotted against the level of inaccuracy in the force vector. The results are shown in Fig. 8.

Figs. 8(a), 8(b), 8(c) and 8(d) indicate the variation of modal mass and damping, stiffness and damping ratio with inaccuracy in force vector respectively. Figs. 8(e) and 8(f) illustrate the coefficients of cubic stiffness non-linearity in the first and second mode. It may be seen that still the error in the modal parameters is not significant because both modes are included in the fit.

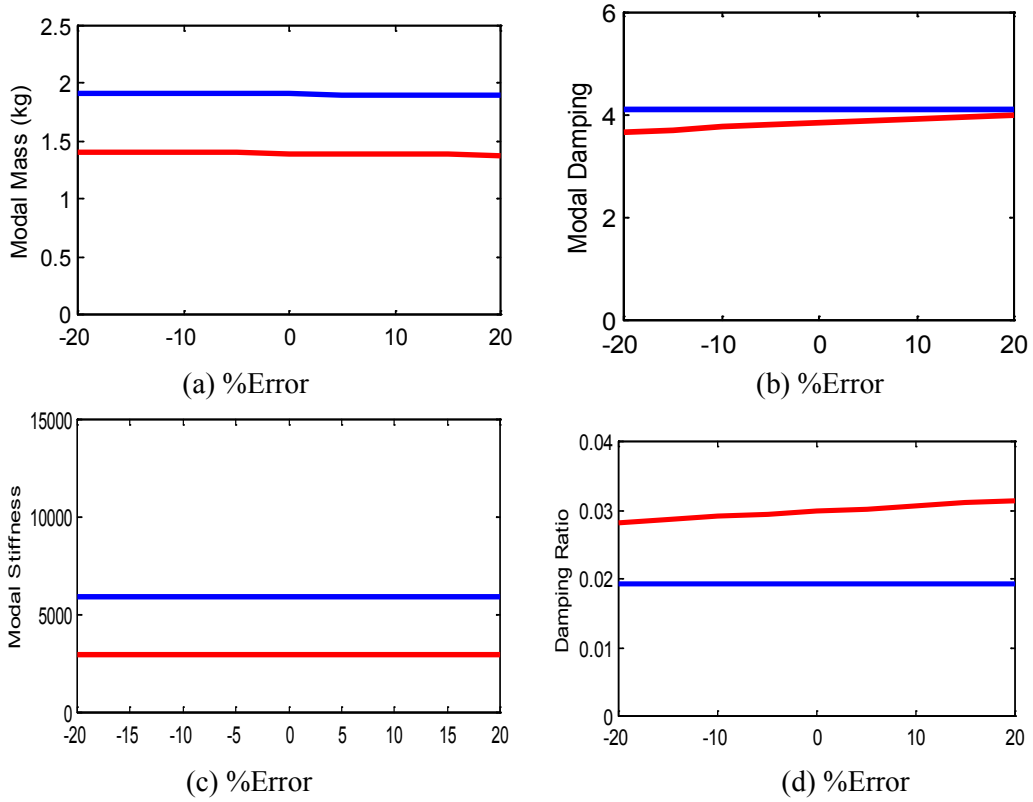

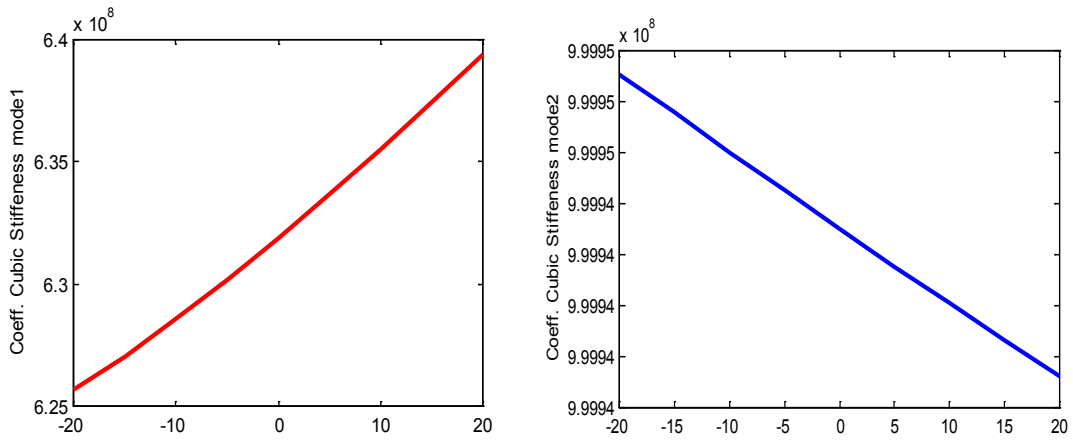

(e) %Error (f) %Error

Figure 8: Variations with inaccuracy on force vector-red (mode 1) and blue (mode 2) a) modal mass b) modal damping c) modal stiffness d) damping ratio e) cubic stiffness non-linearity on mode 1 f) cubic stiffness non-linearity on mode 2

3.2 Inaccuracy in Natural Frequency

Errors in natural frequency calculations arise primarily through an inaccurate MMIF or parameter estimation. A low resolution or noisy MMIF can lead to imprecise identification of natural frequency. Since high levels of noise can occur, and this can lead to particularly inaccurate MMIFs; it is important to monitor and control noise levels for accurate natural frequency identification. If hard tuning is employed, then using an imperfect force vector or inadequate placement or a number of exciters in the normal mode tuning process will lead to errors in natural frequency, as will testing at too high a level and encountering non-linear effects in the FRF or MMIF.

Natural frequency errors could also arise in parameter estimation due to noise on the FRF estimated from the initial test at a low level of excitation or using of an incorrect fitted model. If the frequency is in error, then the system will not be excited at exactly the un-damped natural frequency and so the appropriated force vector may not isolate the modes adequately. If the damping is proportional, it is shown that the force vector is capable of isolating a normal mode at frequencies other than the un-damped natural frequency. However, for a non-proportionally damped system, the force vector only isolates a normal mode when the excitation frequency is exactly equal to the natural frequency. The level of inaccuracy is varied between ± 20% of the exact natural frequency, applied to the natural frequency used in the initial stage, before the Runge-Kutta integration of the burst (the frequency is that used for the force vector). The results are shown graphically in Fig. 9.

Figs. 9(a)-9(f) indicate variations of modal mass, damping, stiffness, damping ratio, coefficient of non-linearity in modes one and two respectively, with inaccuracies in natural frequency. The results show more effects of inaccuracy in natural frequency.

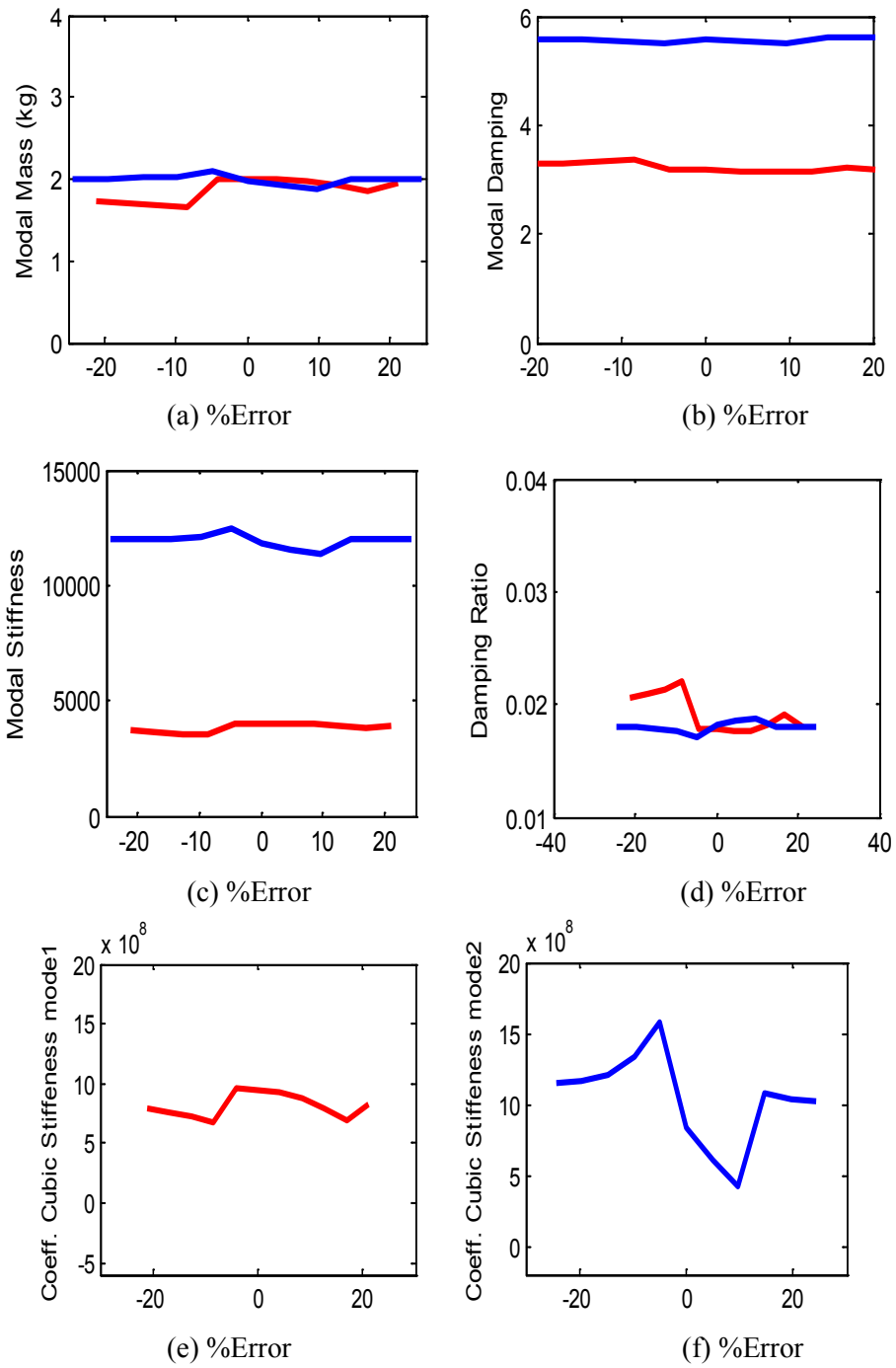

Figure 9: Variations with inaccuracy on natural frequency-red (mode 1) and blue (mode 2) a) modal mass b) modal damping c) modal stiffness d) damping ratio e) cubic stiffness non-linearity on mode 1 f) cubic stiffness non-linearity on mode 2

4 Experimental Case Study

The previous section has discussed the theoretical behaviour of NL-RDM in 2DOF non-linear simulated system. In this section a practical evaluation of this method is explored and discussed. The structure used for testing non-linearity is depicted in Fig. 10. The experimental structure is then tested for evaluation via the NL-RDM. The system is identified, and the values obtained for physical mass,

damping, stiffness and non-linear terms for any cubic stiffness non-linearity present. The results obtained from experimentation are compared to modal parameter results (identified parameters).

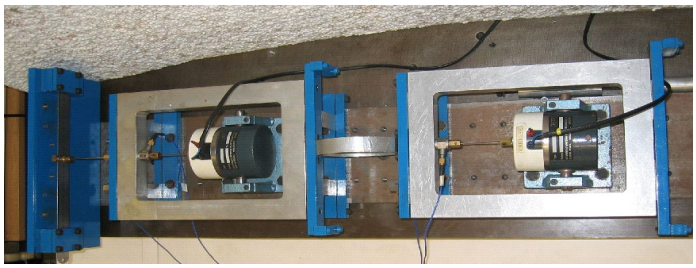

Figure 10: Experimental structure (2DOF NL System)

4.1 Test Setup

Fig. 11 shows the schematic arrangement of the rig adopted for testing. It consists of two mass elements, each connected to a shaker, and connected to each other by a ring; one mass is connected to the clamped-clamped beam to introduce non-linear cubic stiffness. Each mass is supported with flexures to provide a linear stiffness to ground. Damping tape is added to the flexures and ring to increase the damping. The masses were designed to allow the shakers to be incorporated easily without the applied forces being offset.

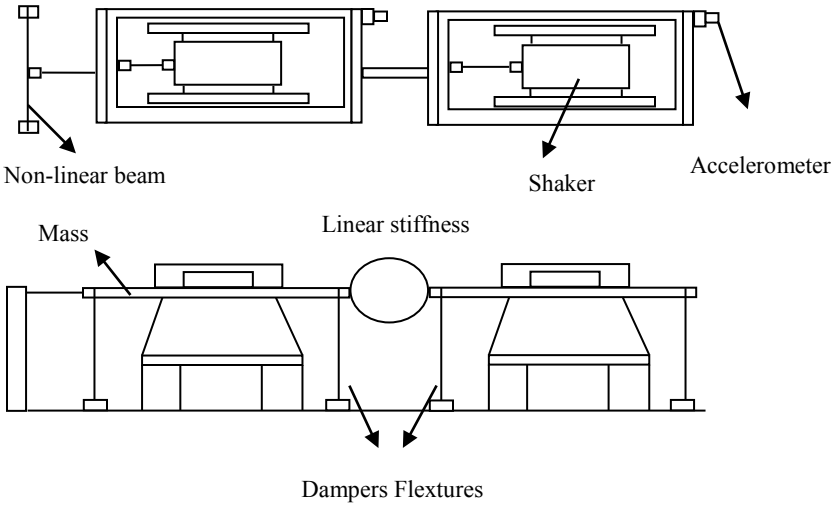

Figure 11: Schematic arrangement of the structure (2DOF NL System)

Accelerometer and shaker positions are shown for all parts in a photo in Fig. 11. Measurements of force and acceleration were taken using two PCB208B force gauges (approximately 100 mV/N), connected to the shakers at their point of action in the masses, and two PCB336 accelerometers (approximately 100 mV/g) respectively; a PCB signal conditioning amplifier was used. The shakers used were Gearing and Watson GWV4, able to generate a maximum force of 18 N. Two 30 Watt current-controlled power amplifiers (one for each shaker) were used to amplify the excitation signal generated by the digital to analogue converter (DAC) prior to input to the shakers. The amplifier was switched to constant current mode to minimise any force drop-out. The dynamic test equipment of Leuven Measurement Systems (LMS) was available in the laboratory, incorporating LMS CADA-X software and LMS-DIFA Scadas II 12 channel acquisition hardware. The hardware configuration includes a high speed

12 bit analogue to digital converter, multiple acquisition channels with programmable dual filtering, and four channels of signal generation via a DAC.

4.2 2DOF Non-linear System

The 2DOF test structure used in this study is based on that described in Eq. (6). A schematic diagram for the 2DOF system with grounded cubic stiffness non-linearity is shown in Fig. 1. Note that this model will yield non-linear behaviour in both modes, and non-linear modal coupling. A summary of all the estimated physical parameters is shown in Tab. 2.

Table 2: Results for physical parameters

Parameter	M_1	M_2	C_1	C_2	K_1	K_2	K_3	Cubic stiffness coefficient
Unit	kg	kg	Ns/m	Ns/m	N/m	N/m	N/m	N/m^3
Physical space	2.61	2.99	7.11	11.06	27057	8401	38226	2.68e + 9

Tab. 3 shows the natural frequencies and mode shapes for the physical model based on the estimated physical parameters in Tab. 2.

Table 3: Mode shapes and natural frequencies derived from physical parameters

Mode shape	DOF1	DOF2	Natural frequency
1	1	0.669	17.00 Hz
2	-0.764	1	21.22 Hz

FRFs were measured using multiple uncorrelated random excitations, for QDAC drive signal levels of 0.25, 0.50, 1.0, 2.0 and 4.0 V, to initially test the structure in the range of 15-25 Hz. Results from these tests are shown in Figs. 12 and 13. The results from these tests may be used to check linearity at low levels and the effect of non-linearity at high levels, via homogeneity.

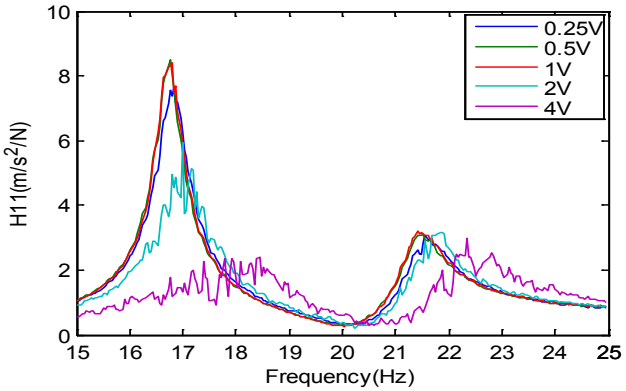

Figure 12: FRF H_{11} at random excitation levels of 0.25, 0.5, 1, 2 and 4 volts

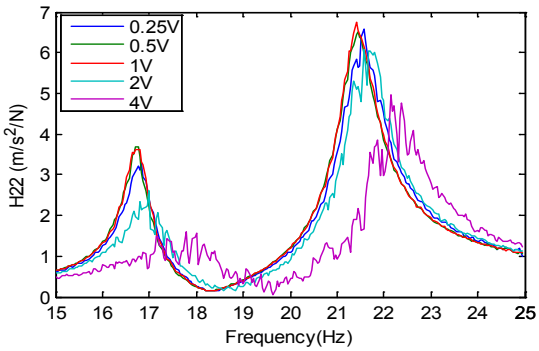

Figure 13: FRF H_{22} at random excitation levels of 0.25, 0.5, 1, 2 and 4 volts

4.3 NL-RDM Test Process

When the rig was tested at a low level of random excitation, the system showed linear and relatively noise-free behaviour. Thus, initially, using the Least Squares Complex Exponential (LSCE) curve fitting method in the LMS software, the natural frequencies, damping ratio and mode shapes for each of the two modes may be estimated. The specific experimental results obtained through the LMS system for the first and second modes respectively are: natural frequencies: 16.87 Hz and 21.53 Hz. damping ratios are 1.45% and 1.86%. Mode shape for mode 1 is $\begin{Bmatrix} 1 \\ 0.662 \end{Bmatrix}$, and for mode 2 is $\begin{Bmatrix} -0.663 \\ 1 \end{Bmatrix}$. Modal masses: 4.54 kg and 4.33 kg. Modal damping: 13.98 kg/s and 21.79 kg/s. Modal linear stiffness: 50990 N/m and 79290 N/m. The natural frequencies and mode shapes agree reasonably well with those in Tab. 3 for the estimated physical parameters.

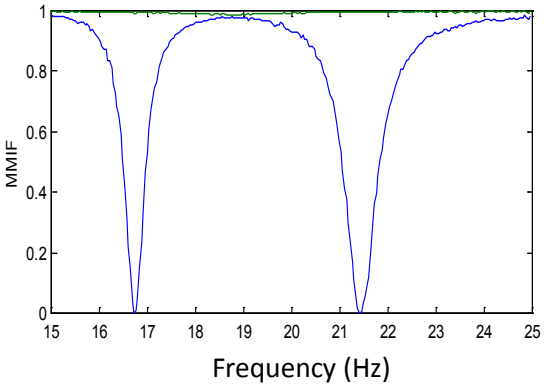

Figure 14: MMIF for low level of excitation (0.5 V)

Next, the MMIF approach was used to process the FRF matrix for the 2DOF non-linear system in order to determine the force vectors required to excite each normal mode of the system at low excitation levels. The dips in the eigenvalues occur at the two un-damped natural frequencies as seen in Fig. 14, when the system was subjected to a low level of excitation (0.5 V). The appropriated force vectors obtained from the linear data are shown in Tab. 4.

Table 4: Force pattern and natural frequency derived from force appropriation

Mode	Effective natural frequency (HZ)	Appropriated force vector	
		Force 1	Force 2
1	16.87	1	0.435
2	21.53	-0.336	1

Next, normal mode tuning was attempted for these two modes in order to determine the voltage patterns required to drive each mode in the burst appropriation stage. The tuned responses are shown in Fig. 15 to indicate the response being near quadrature to force as expected. The tuned mode shapes and natural frequencies for both modes are derived. Tab. 5 shows the results.

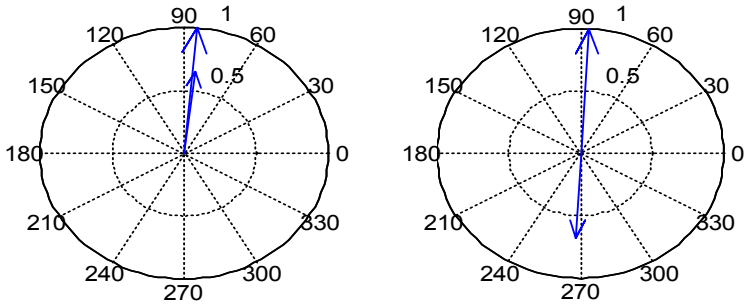

Figure 15: Normal mode tuning mode 1 and 2, by experimental results

Table 5: Tuned natural frequency and mode shape derived from normal mode tuning

Mode	Tuned natural frequency (HZ)	Mode shape	
		Mode 1	Mode 2
1	16.76	1	0.66
2	21.44	-0.675	1

The force excitation was delivered to the system in bursts at the two natural frequencies using the appropriate voltage pattern. In order to excite non-linear behaviour, higher force levels were applied and thus the force appropriation would be imperfect. The data were then being transformed to modal space using a modal matrix. Fig. 16 shows the modal forces for the two modes when seeking to excite mode 1. The imperfect appropriation is seen in the presence of a mode 2 force. Fig. 17 shows the corresponding modal displacement responses; both modes respond, partly due to imperfect appropriation, and partly due to the expected non-linear modal coupling.

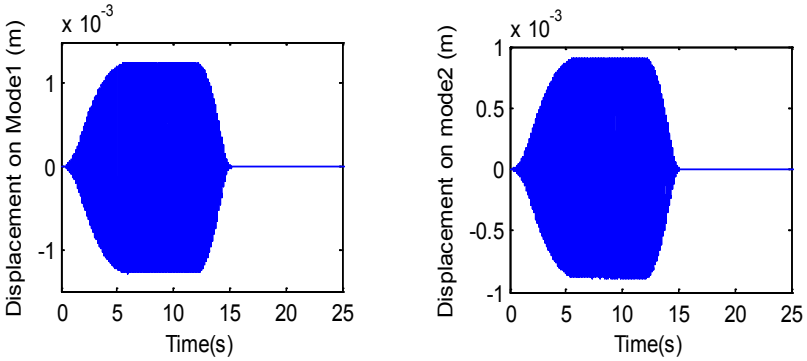

Figure 16: Modal forces for both modes when exciting mode 1

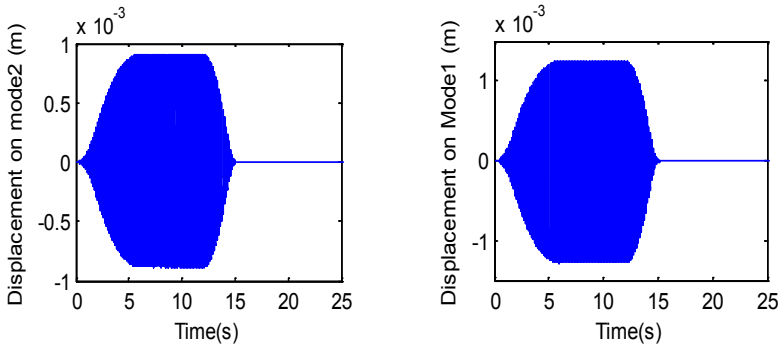

Figure 17: Modal displacement response for both modes when exciting mode 1

If the modal mass is assumed to be known in Eq. (3), then

$$[c]\{\dot{p}\}+[k_L]\{p\}+\{f_{NL}\}=\{f(t)\}-[m]\{\ddot{p}\} \tag{9}$$

where the left hand side of the equation defines the linear and non-linear restoring forces which can be calculated when the modal mass is assumed. The modal restoring force-modal displacement graph shown in Fig. 18 for the first mode demonstrates a reasonably acceptable degree of stiffening non-linearity. The graphs are shown in Fig. 19 for the second mode in 2-D view and here the non-linearity is noticeable but less prominent than for the first mode; this is perhaps not surprising since the modal displacement at the non-linear spring is smaller than for mode 1. Both of these restoring forces show the entire data recorded.

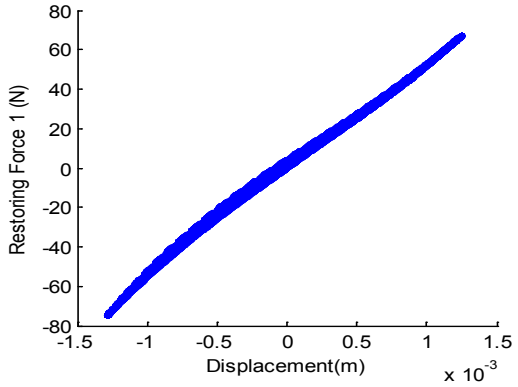

Figure 18: Restoring force-displacement for mode 1

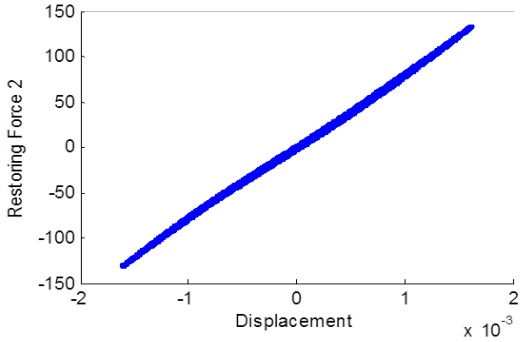

Figure 19: Restoring force-displacement for mode 2

Through curve fitting all unknown parameters except modal mass, then modal damping and linear and non-linear modal stiffness may be identified. The MSE plots for both modes where mass is assumed are shown in Figs. 20 and 21; again it is not simple to decide what model order to assume. The model

order was limited to 3 terms (one linear and two non-linear) because for a higher model order, some coefficients became the wrong sign.

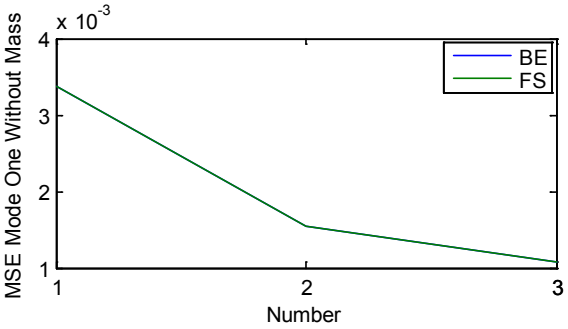

Figure 20: MSE for mode 1 BE and FS least square curve fitting-mass assumed

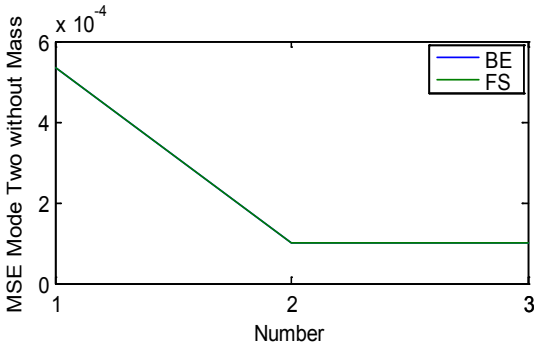

Figure 21: MSE for mode 2 BE and FS-least square curve fitting-mass assumed

In the same way as explained earlier in the last section, the results presented here were considered to have just 2 elements of cubic non-linearity, i.e., 3 elements are included for curve fitting. The results are tabulated in Tab. 6 and they indicate the same results for BE and FS. The values obtained are sensible and will be seen later to agree fairly well with the results obtained from physical parameters.

Table 6: Results for both modes of the system, identified parameters except mass

Parameter	Backward Elimination		Forward Selection	
	Mode 1	Mode 2	Mode 1	Mode 2
c (kg/s)	9.4556	8.6774	9.4556	8.6774
k (N/m)	47392	75809	47392	75809
k Cubic (3,0)	5.44e + 9	0	5.44e + 9	0
k Cubic (2,1)	0	0	0	0
k Cubic (1,2)	0	-4.08e + 9	0	-4.0846e + 9
k Cubic (0,3)	0	0.33e + 9	0	0.32702e + 9

To allow comparison between the two representations, measured parameters and identified NL-RDM parameters, it is necessary to transform the measured physical parameters in Tab. 2 to modal space. Tab. 6 shows the identified parameters for both modes, where the modal masses are assumed as known. Those data from Tab. 6 should be compared to Tab. 7 where the physical model is converted to modal space form.

Table 7: Results for both modes of the measured parameters

Modal parameters	Mode 1	Mode 2
m (kg)	3.95	4.51
c (kg/s)	12.05	15.21
k (N/m)	45091	80166
k Cubic (3,0)	2.68e + 9	-2.05e + 9
k Cubic (2,1)	-6.14e + 9	4.69e + 9
k Cubic (1,2)	4.69e + 9	-3.59e + 9
k Cubic (0,3)	-1.19e + 9	0.91e + 9

To allow comparison between the two representations, measured parameters and identified NL-RDM parameters, it is necessary to transform the measured physical parameters in Tab. 2 to modal space. Tab. 6 shows the identified parameters for both modes, where the modal masses are assumed as known. Those data from Tab. 6 should be compared to Tab. 7 where the physical model is converted to modal space form. As an example, the modal masses identified for the underlying linear model using LSCE are 4.54 kg and 4.33 kg for modes one and two respectively. However, the modal masses from direct physical measurement are calculated as 3.95 kg and 4.51 kg. The mass results show around 4% to 12% error, which is acceptable. Part of the difference may be due to the way in which the mass of the rulers were apportioned; also modal mass is not an easy parameter to identify accurately. The linear modal stiffness for the two modes was 47392 N/m and 75809 N/m from NL-RDM and 45091 N/m and 80166 N/m from direct measurement. These results also indicate good agreement between those linear parameters. However, the difference in these results occurs because of differences in modal mass, since the natural frequency is usually estimated fairly accurately by system identification methods.

The damping values for mode 1 were 9.45 Ns/m (identified from NL-RDM) and 12.05 Ns/m from the underlying linear model and the equivalent values for mode 2 were 8.67 and 15.21 Ns/m respectively. Given how difficult damping is to identify accurately, this agreement is reasonable by considering the point that these values are obtained from non-linear and linear methods and data. The direct cubic stiffness term for the identified mode 1 using NL-RDM was 5.44e9 N/m^3 compared to the value of 2.68e9 N/m^3 from direct measurements; although a factor of 2 is in error, the agreement is reasonably encouraging considering the point that the restoring force surface does not show very much non-linear behaviour. The other terms were omitted from the identified model.

For the second mode, the direct cubic stiffness term for the identified mode 2 using NL-RDM was 0.33e9 N/m^3 compared to 0.91e9 N/m^3 from direct measurements; although a factor of 3 is in error, the restoring force curve showed little non-linearity. Therefore, to some extent it is encouraging that the correct sign and order of magnitude were obtained. The cross-coupling coefficient for the $p_1 p_2^2$ term in mode 2 equation was -4.08e9 N/m^3 from NL-RDM and -3.59e9 N/m^3 from measurements; again this agreement is good. The other coupling terms were not included in the identified model. Thus the 2DOF system with an attached non-linear beam has shown some encouraging agreement between identified and measured parameters.

4.3.1 Sensitivity to Noise

The levels of noise present in the experimental results during system identification are estimated and the sensitivity to noise is considered. To calculate noise as a percentage of the signal generated by NL-RDM, the Root Mean Square (RMS) parameter was estimated from the results generated. The equation used to calculate RMS is as follows:

$$RMS = \sqrt{\frac{1}{n}\sum_{i=1}^{n}\left(p_i(n)\right)^2} \tag{10}$$

where n is the number of data points and p_i is the i^{th} data point. The RMS can be applied to the burst for the acceleration, force or displacement, in either modal or physical space. In order to estimate the signal-to-noise ratio for the burst, two sections of data were compared, namely a section in the 'noise floor' had decayed after the burst, with a section in the maximum part of the burst during the steady state phase of the excitation. The comparison was defined as a percentage

$$RMS_{Noise\_to\_Signal} = \frac{RMS_{Noise}}{RMS_{Signal}} \times 100\% \tag{11}$$

The RMS can be calculated for each mode in the system. In this 2 DOF non-linear model, two $RMS_{Noise\_to\_Signal}$ values were calculated and found to be 0.098% and 0.067% for the modal displacement of the first and second mode respectively. Although no averaging was used in the test, filtering was applied prior to the Fourier transform. The experimental results were poor when the modal mass needed to be identified and this may partly be to do with the noise level. However, when the modal mass was assumed, the results were much better. Thus it would seem that using filtering and an assumed modal mass is sufficient to keep noise effects to a manageable level. The use of a sine wave for the excitation is very helpful in keeping the noise to signal ratio at reasonable levels. The above data was just considered for modal displacement; however, Tab. 8 indicates the results for other variables such as modal force, modal velocity and modal acceleration. In all cases the noise levels were similar to those for displacement.

Table 8: Signal to noise ratio (%) for both modes of modal force, displacement, velocity and acceleration

Mode	Modal Force	Modal Displacement	Modal Velocity	Modal Acceleration
1	0.2141	0.0976	0.1006	0.1144
2	0.2282	0.0669	0.0722	0.0916

5 Conclusions

This paper has presented a complete application of the NL-RDM. The NL-RDM was shown to be a non-linear system identification approach, which essentially combined force appropriation, the RDM and the restoring force surface method based on a modal space. The aim was to identify a model in modal space without requiring large order identification with many modes in a single fit. In this work, the NL-RDM has been applied to a simple 2DOF non-linear system as an illustration of the approach. Moreover, an experimental structure has been identified using the method. Different types of error were accounted for, including the effects of experimental errors in the various early stages of NL-RDM, namely mode shape, force vector, natural frequency, inaccuracy and sensitivity to noise. The results showed that the proposed method is able to identify the non-linear dynamic systems with an acceptable accuracy and this method may provide a practical solution to a difficult problem.

References

1. Billings, S. A., Leontaritis, I. J. (1985). Input-output parametric models for non-linear systems. *International Journal of Control, 41(2),* 329-344.
2. Chapra, S. C., Canale, R. P. (2005). *Numerical methods for engineers*, 5th. McGraw-Hill.
3. Fuellekrug, U., Goege, D. (2012). Identification of weak non-linearities within complex aerospace structures. *Aerospace Science and Technology, 23(1),* 53-62.
4. Gifford, S. J., Tomlinson, G. R. (1989). Recent advances in the application of functional series to non-linear structures. *Journal of Sound and Vibration,135(2),* 289-317.
5. Kerschen, G., Worden, K., Vakakis, A. F., Golinval, J. C. (2006). Past, present and future of non-linear system identification in structural dynamics. *Mechanical Systems and Signal Processing, 20(3),* 505-592.
6. Londoño, J. M., Cooper, J. E., Neild, S. A. (2015). Identification of backbone curves of nonlinear systems from resonance decay responses. *Journal of Sound and Vibration, 384,* 224-238.
7. Lenaerts, V., Kerschen, G., Golinval, J. C. (2001). Proper orthogonal decomposition for model updating of non-linear mechanical systems. *Mechanical Systems and Signal Processing, 15(1),* 31-43.
8. Londoño, J. M., Cooper, J. E., Neild, S. A. (2017). Identification of systems containing non-linear stiffnesses using backbone curves. *Mechanical Systems and Signal Processing, 84,* 116-135.
9. Masri, S. F., Sassi, H., Caughey, T. K. (1982). Non-parametric identification of nearly arbitrary non-linear systems. *Journal of Applied Mechanics, 49(3),* 619-628.
10. Noël, J. P., Kerschen, G. (2017). Non-linear system identification in structural dynamics 10 more years of progress. *Mechanical Systems and Signal Processing, 83,* 2-35.
11. Naylor, S., Platten, M. F., Wright, J. R., Cooper, J. E. (2004). Identification of multi degree of freedom systems with non-proportional damping using the resonant decay method. *ASME Journal of Vibration and Acoustics, 126(2),* 298-306.
12. Platten, M. F., Wright, J. R., Dimitriadis, G., Cooper, J. E. (2007). Identification of multi-degree of freedom non-linear system using an extended modal space model. *Mechanical Systems and Signal Processing, 23,* 8-29.
13. Platten, M. F., Wright, J. R., Cooper, J. E., Dimitriadis, G. (2009). Identification of a non-linear wing structure using an extended modal model. *Journal of Aircraft, 46(5),* 1614-1626.
14. Platten, M. F., Wright, J. R., Cooper, J. E., Sarmast, M. (2002). Identification of multi-degree of freedom non-linear simulated and experimental systems. *Proceedings of the International Conference on Noise and Vibration Engineering,* 1195-1202.
15. Sarmast, M. (2005). *Identification of non-linear dynamic Systems using the non-linear resonant decay method (NL-RDM).* University of Manchester.
16. Shaw, W., Pierre, C. (1993). Normal modes for non-linear vibratory systems. *Journal of Sound and Vibration, 164(1),* 85-124.
17. Vakakis, A. F., Manevitch, L. I., Mikhlin, Y. V., Pilipchuk, V. N., Zevin, A. A. (1996). *Normal modes and localisation in non-linear systems*. Series in Non-linear Science, John Wiley.
18. Worden, K., Tomlinson, G. R. (2001). *Non-linearity in structural dynamics.* Institute of Physics Publishing.
19. Wright, J. R., Platten, M. F., Cooper, J. E., Sarmast, M. (2001). dentification of multi-degree-of-freedom weakly non-linear systems using a model based in modal space. *Proceedings of the International Conference on Structural System Identification.*
20. Wright, J. R., Platten, M. F., Cooper, J. E., Sarmast, M. (2003). Experimental identification of continuous non-linear systems using an extension of force appropriation. *Proceedings of the 21st International Modal Analysis Conference*.
21. Williams, R., Crowley, J., Vold, H. (1985). The multivariate mode indicator function in modal analysis. *Proceedings of the 3rd International Modal Analysis Conference*.